Acta Cryst. (1997). A53, 28–34

An Algorithm for Solving Multiple-Wave Dynamical X-ray Diffraction Equations

YURI P. STETSKO[a] AND SHIH-LIN CHANG[b,c]*

[a]*Chernovtsy State University, Chernovtsy 274012, Ukraine,* [b]*Synchrotron Radiation Research Center, Hsinchu, Taiwan 3007, and* [c]*Department of Physics, National Tsing Hua University, Hsinchu, Taiwan 30043. E-mail: slchang@alpha1.srrc.gov.tw*

(Received 21 March 1996; accepted 17 July 1996)

Abstract

An algorithm is proposed for solving the fundamental equations of the wavefield for multiple-wave dynamical X-ray diffraction with grazing incidence and scattering geometry. The algorithm is developed based on the representation of the electric fields and wavevectors in a single Cartesian coordinate system with one of the axes in the direction normal to the crystal surface. With this representation, the fundamental equations of the wavefield can be solved as an eigenvalue–eigenvector problem involving a $4N \times 4N$ scattering matrix in which the matrix elements are not related to the polarization, N being the number of waves. The polarization factors are absorbed in the vector components of the eigenvectors. This simplifies the process in solving the fundamental equation, avoids unnecessary approximations on polarization in the matrix calculation and makes the algorithm very generic so that it can be applied to multiple diffractions of all kinds, including grazing-angle and wide-angle geometries. The intensity distribution of an *Umweganregung* of a specularly diffracted wave in a polarization-forbidden state is calculated using this algorithm as a demonstration.

1. Introduction

Specular X-ray reflections by a crystal surface are usually not accounted for in conventional X-ray diffraction theory for cases where the angles between the incident and/or scattered wavevectors and the crystal surface are large compared with the critical angle for total external reflection. In these cases, the linearization of the resonance term

$$(k_h^3 - K^2)/k_h^2 \simeq (k_h^2 - K^2)/K^2 \simeq 2(k_h - K)/K \equiv \varepsilon_h \tag{1}$$

in the dispersion relation is usually adopted in the conventional dynamical theory (von Laue, 1931; Pinsker, 1978), where K and k_h are the magnitudes of the incident wavevector $\mathbf{K}$ in vacuum and the diffracted wavevector $\mathbf{k}_h$ inside the crystal and $\mathbf{k}_h = \mathbf{k}_0 + \mathbf{h}$, $\mathbf{h}$ being the reciprocal-lattice vector of the h reflection and $\mathbf{k}_0$ is the wavevector in the incident direction inside the crystal. The transformation of a system of vector equations to that of scalar equations is often carried out by introducing mutually orthogonal unit vectors $\boldsymbol{\sigma}_h$, $\boldsymbol{\pi}_h$ and $\mathbf{s}_h = \mathbf{k}_h/k_h$, $\boldsymbol{\sigma}_h$ and $\boldsymbol{\pi}_h$ being the polarization vectors perpendicular and parallel to the plane of incidence of the h reflection. As was shown by Kohn (1979) and many others, for N strong waves, the fundamental equations can be solved as an eigenvalue equation in a $2N \times 2N$ scattering-matrix form, where the unknowns are the eigenvalues ε_h in the diagonal and the scalar products of the polarization unit vectors, say $(\boldsymbol{\sigma}_h \cdot \boldsymbol{\sigma}_{h'})$, $(\boldsymbol{\sigma}_h \cdot \boldsymbol{\pi}_{h'})$, $(\boldsymbol{\pi}_h \cdot \boldsymbol{\pi}_{h'}), \ldots$ in the off-diagonal elements. As the modulus of the normal component s_h to the crystal surface is small, of the order of the Fourier component of the crystal polarizability, $\chi_h \simeq 10^{-5}$, the scalar products can be obtained by assigning the origins of the wavevectors in the vicinity of the multiple-wave Lorentz point, thus reducing the error in ε_h.

This process of linearization of the dispersion equation leaving out $2N$ solutions associated with specularly reflected and specularly diffracted waves is no longer valid for diffractions at grazing angles. It is then necessary to take into account the quadratic terms in the dispersion equation and the refractive indices in the boundary conditions. This has been done by Kishino & Kohra (1971) for two-beam diffractions, by Andreev, Gorshkov & Ilinskiy (1985), Hung & Chang (1989), Stepanov, Kondrashkina & Novikov (1991) and Tseng & Chang (1990) for some special cases, and by Colella (1974) and Stepanov & Ulyanenkov (1994) for a general case.

The approach taken by Colella (1974) is again based on the introduction of unit vectors $\boldsymbol{\sigma}_h$ and $\boldsymbol{\pi}_h$ normal to the wave vector $\mathbf{k}_h$. The solution then amounts to finding the eigenvalues and eigenvectors of a $4N \times 4N$ scattering matrix whose unknown elements $(\boldsymbol{\sigma}_h \cdot \boldsymbol{\sigma}_{h'})$, $(\boldsymbol{\sigma}_h \cdot \boldsymbol{\pi}_{h'})$, $(\boldsymbol{\pi}_h \cdot \boldsymbol{\pi}_{h'})$ are also dependent on the approximation used to obtain $\mathbf{s}_h$. The principal feature of the grazing-angle diffraction is that the range of variation of the normal components of $\mathbf{s}_h$ vectors increases dramatically as the incident or scattered angle decreases and reaches $(\chi_h)^{1/2} \simeq 10^{-2}$–$10^{-3}$ near the critical angle so that any choice of the linear approximation in ε_h will lead to errors in $(\boldsymbol{\sigma}_h \cdot \boldsymbol{\sigma}_{h'})$,

$(\boldsymbol{\sigma}_h \cdot \boldsymbol{\pi}_{h'})$, $(\boldsymbol{\pi}_h \cdot \boldsymbol{\pi}_{h'})$ comparable to $(\chi_h)^{1/2}$. Consequently, errors in determining the amplitude values and even in the signs of the imaginary parts of the eigenvalues may occur when the latter tend to zero. This approach thus requires successive approximations for each root or group of related roots of the dispersion equation until the required accuracy is achieved (Gau & Chang, 1995). This increases greatly the amount of time required for computations. In a modification of Colella's method proposed by Stepanov & Ulyanenkov (1994), some of the waves undergo grazing-angle diffraction, and the specularly diffracted waves that are far enough from the grazing angular position are left out. This approach results in a scattering matrix of size smaller than $4N \times 4N$, thus reducing, when possible, the computation time. This approach, however, still has the same disadvantage as that of Colella.

The idea of the approach proposed here is to represent the amplitudes of the diffracted waves on a basis that would be independent of the unknown wavevectors $\mathbf{k}_h$. The amplitudes and wavevectors are represented in a single Cartesian system of coordinates related to the normal $\mathbf{n}$ to the entrance surface of the crystal. The proposed algorithm then amounts to finding eigenvalues and eigenvectors of the $4N \times 4N$ scattering matrix whose elements are independent of any unknown quantities.

2. Representing the dynamic X-ray diffraction equations in terms of eigenvalues and eigenvectors

When dealing with an N-wave diffraction in grazing-angle geometry, the fundamental equations of wavefield are expressed in terms of the electric field $\mathbf{E}$ as

$$[(k_{h_m}^2 - K^2)/K^2]\mathbf{E}_{h_m} = [(\mathbf{k}_{h_m} \cdot \mathbf{E}_{h_m})/K^2]\mathbf{k}_{h_m} + \sum_{n=0}^{N-1} \chi_{h_m - h_n} \mathbf{E}_{h_n}, \quad (2)$$

where $m = 0, 1, \ldots, N-1$ and $K = 1/\lambda$, λ being the wavelength used (see Fig. 1). Indeed, as noted by Hartwig (1978), for grazing-angle geometry, the normal components of the $\mathbf{E}_h$ and those of the electric displacement $\mathbf{D}_h$ can differ considerably, resulting in a significant error in the normal component $\mathbf{D}_h$.

The tangential components of wavevectors are known to be continuous across the interface between two media. Therefore, the origins of the wavevectors propagating both inside and outside the crystal will lie along the crystal-surface normal $\mathbf{n}$, assuming that the ends of these vectors are in the appropriate reciprocal-lattice sites H_m. Thus, to reduce the system (2) of vector equations to scalar ones, we introduce the following Cartesian coordinate system in the reciprocal space. The z axis is parallel to the external normal $\mathbf{n}$ to the crystal entrance surface. The choice of the origin and the x and y axes is arbitrary, and is governed solely by the convenience of representation of results in each particular case. We designate the coordinates of the reciprocal-lattice sites in the above-mentioned coordinate system as X_m, Y_m, Z_m, and the coordinates of the origins of the wavevectors as x_n, y_n, z. Here, x_n and y_n describing the position of the normal are defined by the angular and spectral parameters of the incident wave while the unknown quantity z is obtained from the dispersion equation.

Substituting the Cartesian representations

$$\mathbf{k}_{h_m} = (X_m - x_n)\mathbf{i} + (Y_m - y_n)\mathbf{j} + (Z_m - z)\mathbf{k} \equiv x_m\mathbf{i} + y_m\mathbf{j} + (Z_m - z)\mathbf{k} \quad (3)$$

and

$$\mathbf{E}_{h_m} = E_m^x\mathbf{i} + E_m^y\mathbf{j} + E_m^z\mathbf{k} \quad (4)$$

into (1), we obtain a system of $3N$ scalar equations. In matrix form, it is given by

$$\mathbf{PE} = \begin{pmatrix} (\mathbf{C} - z\mathbf{I})^2 + \mathbf{B}^2 - \mathbf{G}^2 & -\mathbf{AB} & -\mathbf{A}(\mathbf{C} - z\mathbf{I}) \\ -\mathbf{AB} & (\mathbf{C} - z\mathbf{I})^2 + \mathbf{A}^2 - \mathbf{G}^2 & -\mathbf{B}(\mathbf{C} - z\mathbf{I}) \\ -\mathbf{A}(\mathbf{C} - z\mathbf{I}) & -\mathbf{B}(\mathbf{C} - z\mathbf{I}) & \mathbf{A}^2 + \mathbf{B}^2 - \mathbf{G}^2 \end{pmatrix} \times \begin{pmatrix} \mathbf{E}_x \\ \mathbf{E}_y \\ \mathbf{E}_z \end{pmatrix} = 0, \quad (5)$$

where all the matrices in the system are $N \times N$, $\mathbf{I}$ is the unit matrix, $\mathbf{A}$, $\mathbf{B}$, $\mathbf{C}$ are the diagonal matrices whose diagonal elements are given by $a_{mm} = x_m$, $b_{mm} = y_m$, $c_{mm} = Z_m$, respectively, $\mathbf{G}^2 = K^2(\mathbf{I} + \mathbf{F})$, $\mathbf{F}$ is the matrix whose elements are given by $f_{mm} = \chi_{h_m - h_n}$ and $\mathbf{E}_x = (E_0^x, E_1^x, \ldots, E_{N-1}^x)^T$, $\mathbf{E}_y = (E_0^y, E_1^y, \ldots, E_{N-1}^y)^T$, $\mathbf{E}_z = (E_0^z, E_1^z, \ldots, E_{N-1}^z)^T$ are the vector columns of unknown components of electrical vectors and the superscript T means transpose. We note that $\mathbf{A}$, $\mathbf{B}$, $\mathbf{C}$ matrices are commutative.

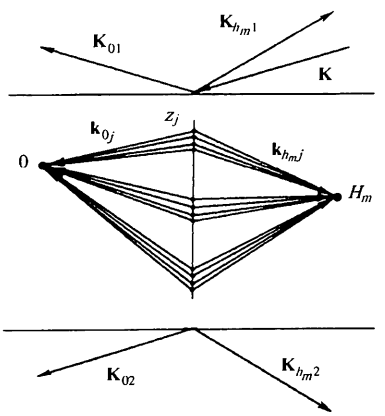

Fig. 1. Schematic representation of multiple X-ray diffraction in a crystal plate.

The unknown z is obtained from the equation $\det \mathbf{P} = 0$, whose left-hand side is a $4N$th-order polynomial.

To reduce the matrix equation (5) to an eigenvalue–eigenvector problem, the following transformations are made. We now introduce new variables

$$\begin{aligned} \mathbf{E}_v &= (\mathbf{C} - z\mathbf{I})\mathbf{E}_x - \mathbf{A}\mathbf{E}_z \\ \mathbf{E}_w &= (\mathbf{C} - z\mathbf{I})\mathbf{E}_y - \mathbf{B}\mathbf{E}_z. \end{aligned} \tag{6}$$

By substituting $\mathbf{E}_v$ and $\mathbf{E}_w$ into system (5), we obtain an extended system of size $5N \times 5N$:

$$\begin{pmatrix} \mathbf{C}-z\mathbf{I} & \mathbf{0} & -\mathbf{I} & \mathbf{0} & -\mathbf{A} \\ \mathbf{0} & \mathbf{C}-z\mathbf{I} & \mathbf{0} & -\mathbf{I} & -\mathbf{B} \\ \mathbf{B}^2-\mathbf{G}^2 & -\mathbf{AB} & \mathbf{C}-z\mathbf{I} & \mathbf{0} & \mathbf{0} \\ -\mathbf{AB} & \mathbf{A}^2-\mathbf{G}^2 & \mathbf{0} & \mathbf{C}-z\mathbf{I} & \mathbf{0} \\ -\mathbf{A}(\mathbf{C}-z\mathbf{I}) & -\mathbf{B}(\mathbf{C}-z\mathbf{I}) & \mathbf{0} & \mathbf{0} & \mathbf{A}^2+\mathbf{B}^2-\mathbf{G}^2 \end{pmatrix} \begin{pmatrix} \mathbf{E}_x \\ \mathbf{E}_y \\ \mathbf{E}_v \\ \mathbf{E}_w \\ \mathbf{E}_z \end{pmatrix} = 0, \tag{7}$$

where $\mathbf{0}$ is the zero matrix. We then eliminate the expression $(\mathbf{C} - z\mathbf{I})$ in the fifth row of system (7) by multiplying the first row to the left by the matrix $\mathbf{A}$, the second row by $\mathbf{B}$, then adding the result to the fifth row. Similarly, we eliminate the off-diagonal elements in the fifth column and, finally, obtain

$$\begin{aligned} (\mathbf{Q} - z\mathbf{I}_4)\mathbf{E}_4 &= 0 \\ \mathbf{E}_z &= -\mathbf{G}^{-2}(\mathbf{A}\mathbf{E}_v + \mathbf{B}\mathbf{E}_w), \end{aligned} \tag{8}$$

where

$$\mathbf{Q} = \begin{pmatrix} \mathbf{C} & \mathbf{0} & \mathbf{A}\mathbf{G}^{-2}\mathbf{A} - \mathbf{I} & \mathbf{A}\mathbf{G}^{-2}\mathbf{B} \\ \mathbf{0} & \mathbf{C} & \mathbf{B}\mathbf{G}^{-2}\mathbf{A} & \mathbf{B}\mathbf{G}^{-2}\mathbf{B} - \mathbf{I} \\ \mathbf{B}^2 - \mathbf{G}^2 & -\mathbf{AB} & \mathbf{C} & \mathbf{0} \\ -\mathbf{AB} & \mathbf{A}^2 - \mathbf{G}^2 & \mathbf{0} & \mathbf{C} \end{pmatrix}, \tag{9}$$

the column $E_4 = [(E_x)^T, (E_y)^T, (E_v)^T, (E_w)^T]^T$ contains no normal components E_z and $\mathbf{I}_4$ is the $4N \times 4N$ unit matrix. As is seen from the first matrix equation of system (8), the problem has been reduced to finding the eigenvalues z_j and eigenvectors of the $\mathbf{Q}$ matrix, whose elements are independent of z. The first and second N components of the eigenvalues are, within the accuracy of the proportionality constants c_j, the x and y components of the amplitudes of the diffracted waves. These proportionality constants can be found from the boundary conditions. Then, the term $\mathbf{E}_z$ can be calculated from the second equation of the system (8) using the third and fourth N components of the eigenvector.

For some special diffraction cases, a simplified solution of the dynamical X-ray diffraction equations is possible. Consider the case where all the Z_m ($m = 0, 1, \ldots, N-1$) of the reciprocal-lattice sites are equal. In this case, all the reflecting planes will be normal to the entrance surface. Without loss of generality, we assume $Z_m = 0$. We eliminate the off-diagonal elements in the third row of the system (5) by multiplying the first row to the left by the matrix $\mathbf{A}$, the second row by $\mathbf{B}$, then add the result to the third row multiplied by $-z\mathbf{I}$. We then eliminate the off-diagonal elements in the third column and obtain

$$\begin{aligned} (\mathbf{U} + z^2\mathbf{I}_2)\mathbf{E}_2 &= 0 \\ \mathbf{E}_z &= z^{-1}(\mathbf{G}^{-2}\mathbf{A}\mathbf{G}^2\mathbf{E}_x + \mathbf{G}^{-2}\mathbf{B}\mathbf{G}^2\mathbf{E}_y), \end{aligned} \tag{10}$$

where

$$\mathbf{U} = \begin{pmatrix} \mathbf{A}\mathbf{G}^{-2}\mathbf{A}\mathbf{G}^2 & -\mathbf{AB} + \mathbf{A}\mathbf{G}^{-2}\mathbf{B}\mathbf{G}^2 \\ -\mathbf{AB} + \mathbf{B}\mathbf{G}^{-2}\mathbf{A}\mathbf{G}^2 & \mathbf{A}^2 + \mathbf{B}\mathbf{G}^{-2}\mathbf{B}\mathbf{G}^2 - \mathbf{G}^2 \end{pmatrix}, \tag{11}$$

$\mathbf{I}_2$ is the $2N \times 2N$ unit matrix and the column $\mathbf{E}_2 = [(\mathbf{E}_x)^T, (\mathbf{E}_y)^T]^T$. Thus, the solution of the equations in this particular case is reduced to finding the eigenvalues $-z_j^2$ and eigenvectors of the $2N \times 2N$ scattering matrix $\mathbf{U}$. The solutions are seen to be symmetrical with respect to $z = 0$.

3. Boundary conditions

By making use of the continuity of the normal component and the tangential component of the electric field $\mathbf{E}^T$, the electric displacement $\mathbf{D}^z$ and the magnetic field $\mathbf{H}$ ($\mu = 1$) and invoking the relations $\mathbf{D}_h = \mathbf{E}_h + \sum_{h'} \chi_{h-h'}\mathbf{E}_{h'}$ and $\mathbf{H}_h = [\mathbf{k}_h \times \mathbf{E}_h]/K$, one obtains the following equations for the entrance ($l = 1$) and exit ($l = 2$) surfaces of a plane-parallel crystal plate of thickness t:

$$\begin{aligned} \sum_{j=1}^{4N} c_j E_{mj}^x \psi_{jl} &= E^x \delta_{ml}^{(0)} + E_{ml}^x \varphi_{ml} \\ \sum_{j=1}^{4N} c_j E_{mj}^y \psi_{jl} &= E^y \delta_{ml}^{(0)} + E_{ml}^y \varphi_{ml} \\ \sum_{j=1}^{4N} c_j \left(E_{mj}^z + \sum_{n=0}^{N-1} \chi_{h_m - h_n} E_{nj}^z \right) \psi_{jl} &= E^z \delta_{ml}^{(0)} + E_{ml}^z \varphi_{ml} \\ \sum_{j=1}^{4N} c_j (z_{ml} E_{mj}^y - y_m E_{mj}^z) \psi_{jl} & \\ = (K_m^2 E^y - y_m E^z)\delta_{ml}^{(0)} + [(-1)^l K_m^2 E_{ml}^y - y_m E_{ml}^2]\varphi_{ml} & \\ \sum_{j=1}^{4N} c_j (x_m E_{mj}^z - z_{mj} E_{jl}^x) \psi_{jl} & \\ = (x_m E^z - K_m^z E^x)\delta_{ml}^{(0)} + [x_m E_{ml}^z - (-1)^l K_m^z E_{ml}^x]\varphi_{ml} & \\ \sum_{j=1}^{4N} c_j (y_m E_{mj}^x - x_m E_{mj}^y) \psi_{jl} & \\ = (y_m E^x - x_m E^y)\delta_{ml}^{(0)} + [y_m E_{ml}^x - x_m E_{ml}^y]\varphi_{ml}, & \end{aligned} \tag{12}$$

where

$$\delta_{ml}^{(0)} = \begin{cases} 1 & \text{for } m = 0 \\ 0 & \text{for } m \neq 0 \end{cases} \quad \text{if } l = 1 \qquad \text{if } l = 2, \tag{13}$$

E^x, E^y, E^z are the vector components of the electric field of the incident wave. $E^x_{m1}, E^y_{m1}, E^z_{m1}$ and $E^x_{m2}, E^y_{m2}, E^z_{m2}$ are the vector components of the electric field in front of and behind the crystal, respectively, where $K^z_m = -[K^2 - (x^2_m + y^2_m)]^{1/2}$, $\psi_{j1} = \varphi_{m1} = 1$, $\psi_{j2} = \exp(2\pi i z_{mj} t)$, $\varphi_{m2} = \exp(2\pi i K^z_m t)$ and $Z_{mj} = Z_m - z_j$. The propagation directions inside and outside the crystal are shown in Fig. 1, where the **K**'s are the wavevectors outside the crystal and 0 and H_m are the reciprocal-lattice points of the direct and the H_m reflection, respectively. The normal components of the wave vectors of the outgoing diffracted waves at the entrance surface are given by $K^z_{h_m 1} = -K^z_m$, whereas at the exit surface they are given by $K^z_{h_m 2} = K^z_m$.

The last equation of the system (12) is seen to be a linear combination of the first two. For X-rays, the condition of continuity of the normal components of the magnetic inductions follows from the condition of continuity of the tangential component of the eclectic field. We are thus left with $5N$ linearly independent equations for the entrance and the exit surfaces. The system (12) of linear equations contains $4N$ unknown c_j and $3N$ unknown components of the electric fields of the diffracted waves in front of the crystal and $3N$ unknown components behind the crystal. We thus obtain a system of $10N$ equations with $10N$ unknowns.

It is to be noted that, in the approach of Colella (1974), a system of only $8N$ equations with $8N$ unknowns is involved in the boundary conditions. This is because $2N$ longitudinal components of the vectors $\mathbf{D}_h$ of diffracted waves outside the crystal are not considered. The proposed algorithm of this paper, however, gives a simple way to reduce a system (12) of $10N$ equations to a system of $4N$ equations, containing only constants c_j as the unknowns. This is accomplished by eliminating the unknowns in the right-hand sides of the fourth and fifth equations of the system (12) by multiplying the second equation with $(-1)^{l+1} K^z_m$, the third by y_m, and adding the result to the fourth. We thus end up with the system

$$\sum_{j=1}^{4N} c_j \left\{ [z_{mj} - (-1)^l K^z_m] E^x_{mj} + x_m \sum_{n=0}^{N-1} \chi_{h_m - h_n} E^z_{nj} \right\} \psi_{jl} = 2K^z_m E^x \delta^{(0)}_{ml}$$

$$\sum_{j=1}^{4N} c_j \left\{ [z_{mj} - (-1)^l K^z_m] E^y_{mj} + y_m \sum_{n=0}^{N-1} \chi_{h_m - h_n} E^z_{nj} \right\} \psi_{jl} = 2K^z_m E^y \delta^{(0)}_{ml}. \quad (14)$$

Substituting the determined constants c_j from (14) into the system (12), we finally obtain the vector components of the electric field of the diffracted waves.

Computational solutions for the systems (12) and (14) are only possible for relatively thin crystals, when no overflow in the exponential functions ψ_{j2} occurs. To circumvent this overflow for thick crystals and for semi-infinite crystals ($t \to \infty$), we introduce a new variable

$$p_j = \begin{cases} c_j \psi_{j2} & \text{for Im } z_j > 0 \\ c_j & \text{for Im } z_j \le 0. \end{cases} \quad (15)$$

The boundary conditions, (12) and (14), remain valid, except that now c_j are replaced by p_j and ψ_{jl} are replaced by ξ_{jl}, which are defined as

$$\xi_{jl} = \begin{cases} \left.\begin{matrix} \xi_j & \text{for Im } z_j > 0 \\ 1 & \text{for Im } z_j \le 0 \end{matrix}\right\} \text{ if } l = 1 \\ \left.\begin{matrix} 1 & \text{for Im } z_j > 0 \\ \xi_j & \text{for Im } z_j \le 0 \end{matrix}\right\} \text{ if } l = 2, \end{cases} \quad (16)$$

where $\xi_j = \exp[\text{sign}(\text{Im } z_j) 2\pi i z_j t]$. The systems thus obtained are free from the limitations on $|\xi_j|$ inherent in (12) and (14), which decrease as the crystal thickness increases, and for a semi-infinite crystal $|\xi_j| = 0$. An essentially similar approach was proposed earlier by Kohn (1979).

4. *Umweganregung* of a specularly diffracted wave at a forbidden polarization state

During the dynamical multiwave X-ray interaction, *Umweganregung* (Renninger, 1937) and *Aufhellung* (Wagner, 1923) may occur simultaneously or separately, appearing as a diffracted wave intensity increase or decrease, respectively, as compared with the two-wave case. For weak or structure-forbidden reflections with small values of the structural factors, *Aufhellung* in the multiple-wave region is suppressed, whereas *Umweganregung* becomes more pronounced owing to several consecutive allowed reflections. For a polarization-forbidden reflection, *Umweganregung* was predicted and experimentally observed by Kshevetsky, Stetsko & Sheludko (1985) for an allowed reflection using π-polarized X-rays, with the electric field vector lying in the reflection plane and the diffraction angle θ close to $\pi/4$. The diffracted beam intensity is then close to zero, since it is proportional to $\cos 2\theta$. Although the above-mentioned phenomena were originally observed for the conventional wide-angle X-ray diffraction, similar phenomena can be expected to occur for specularly diffracted waves of grazing-incidence multiple-wave diffraction. Evidence for this is the fact that, in the two-wave case, the amplitudes of both diffracted and specularly reflected waves depend in a similar way on the structure and polarization factors. A theoretical study of *Umwegunregung* in grazing-incidence geometry involving the nearly forbidden reflection has been reported by Tseng & Chang (1990).

In the present section, the calculation results are reported for the *Umwegunregung* involving specularly diffracted waves with forbidden polarization in an Si(000,400,$\bar{2}$64) diffraction. The calculations are made for the three-wave diffraction case in which all the reflecting planes are normal to the entrance surface,

which is parallel to the $(1\bar{1}2)$ planes (see Fig. 2) and all the waves propagate with small angles with respect to the entrance surface. The wavevectors in Fig. 2 have the same meaning as those in Fig. 1 and **n** is the vector normal to the crystal surface. The angles between the wavevectors **K** and the surface are φ. The points 0, H_1 and H_2 shown in Fig. 2(*b*) represent the reciprocal-lattice points of the 000, 440 and $\bar{2}64$ reflections, respectively.

An important feature of multiple-wave interaction of grazing X-ray beams is its coincidental nature. This is in contrast to the well known diffraction cases in which at least three-wave diffraction is of a systematic nature (see, for example, Chang, 1984). The reason is that in the latter no consideration was given to the orientation of the entrance surface. For grazing-incidence diffraction, however, this orientation becomes a significant factor in determining the coincidence of the multiple-wave interaction. It should be noted, however, that a systematic multiple-wave diffraction can be realized for grazing beams as well if the plane of configuration containing all the reciprocal-lattice points involved is normal to the crystal entrance surface.

In view of the coincident nature of the multiple-wave diffraction, the calculations are carried out for different incident wavelengths. The exact multiple-wave diffraction condition is that the multiwave Lorentz point should be in the plane of configuration mentioned. The wavelength satisfying this condition is given by $\lambda_M = 1.34380$ Å and the diffraction angle by $\theta_{440} = 0.77519$ rad, which is close to $\pi/4$. The spectral parameter is taken to be $S = (\lambda - \lambda_M)/\lambda_M$. Figs. 3 and 4 show the variation of angular distributions of the

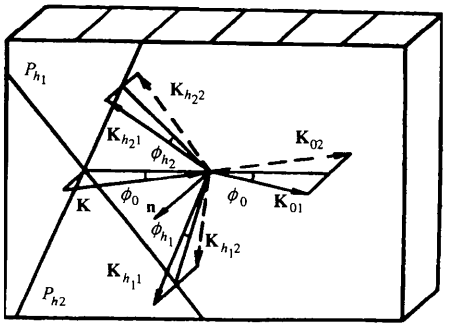

(*a*)

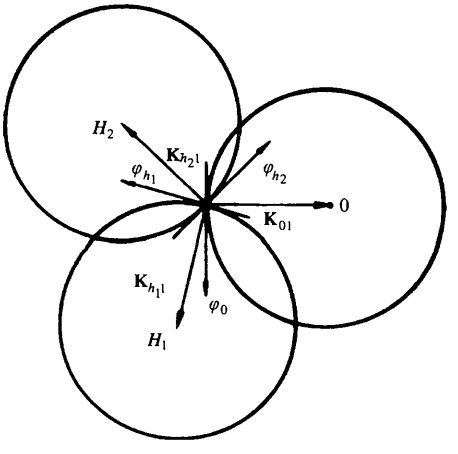

(*b*)

Fig. 2. Geometry of the three-wave X-ray diffraction in (*a*) real space and (*b*) reciprocal space. The vector **n** is along $[1\bar{1}2]$.

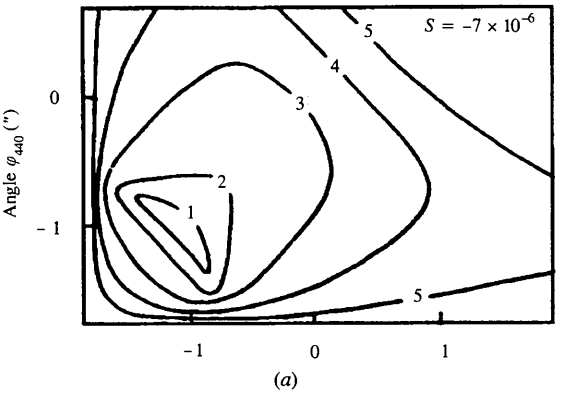

(*a*)

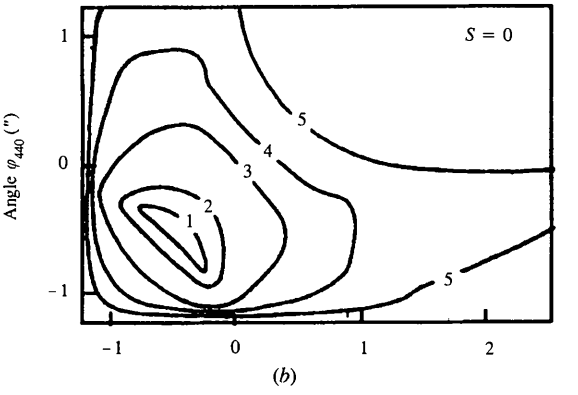

(*b*)

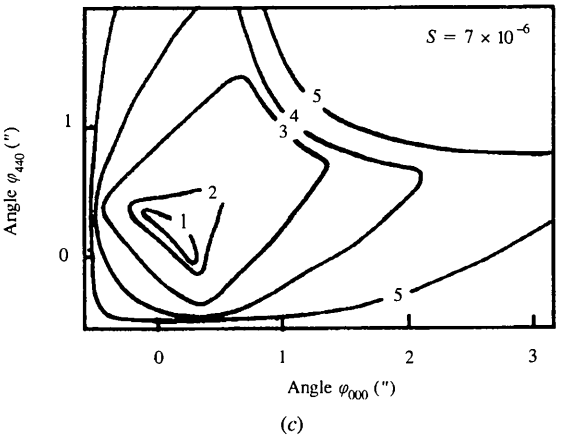

(*c*)

Fig. 3. Reflection coefficient $R_{440}(\varphi_{000}, \varphi_{440})$ for σ-polarized incident radiation. Levels 1–5 correspond to $R_{440} = 0.3$, 0.2, 0.1, 5×10^{-2}, 10^{-2}, respectively.

reflection coefficient $R_{440}(\varphi_{000}, \varphi_{440})$ for a specularly diffracted wave (440) in the vicinity of $S = 0$. The coordinates are chosen at the intersection of the normal **n** and the plane of the configuration, so that the one-wave azimuthal axes φ_{000} and φ_{440} (see Fig. 2*b*) preserve their directions and scales. The origins ($\varphi_{000} = 0, \varphi_{440} = 0$) along the azimuthal axes are chosen so as to correspond to the normal **n** passing through the multiple-wave Lorentz point. When the normal **n** passes through the bisector of the angle between the axes φ_{000} and φ_{440}, the grazing angles ϕ_{000} and ϕ_{440} will be equal. From Figs. 3 and 4, it is evident that, for the σ polarization, the distribution of R_{400} varies slightly as the spectral parameter S changes from -7×10^{-6} to 0 and then to $+7 \times 10^{-6}$, while, for the π polarization, the difference in R_{40} is considerable between $S = 0$ and $S = \pm 7 \times 10^{-6}$. These distinct differences are mainly due to the difference in the polarization direction with respect to the positions of the reciprocal-lattice points.

The estimated bandwidth of the multiple-wave interaction is of the order of $\chi_h \simeq 10^{-5}$. Therefore, an experimental observation of multiple-wave diffraction would require a highly monochromatic incident beam. However, the measurement of the angular distribution of a specularly diffracted wave for the multiple-wave case would still involve considerable difficulties, since such a distribution would be qualitatively indistinguishable from that for the two-wave case. To overcome this difficulty, we propose the method of spectral scanning of the multiple-wave region. One practical way of spectral scanning of the multiple-wave region is as follows. Consider a highly monochromatic beam incident on the crystal surface at a fixed angle ϕ_{000}

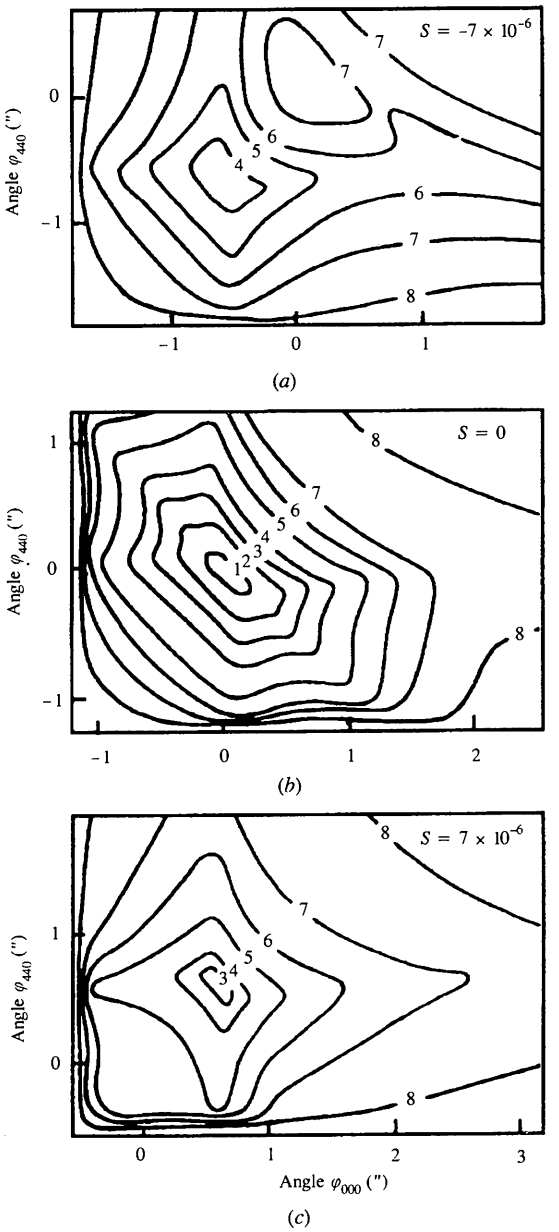

Fig. 4. Reflection coefficient $R_{440}(\varphi_{000}, \varphi_{440})$ for π-polarized incident radiation. Levels 1-8 correspond to $R_{440} = 5 \times 10^{-2}$, 10^{-2}, 5×10^{-3}, 2×10^{-3}, 10^{-3}, 5×10^{-4}, 2×10^{-4}, 10^{-4}, respectively.

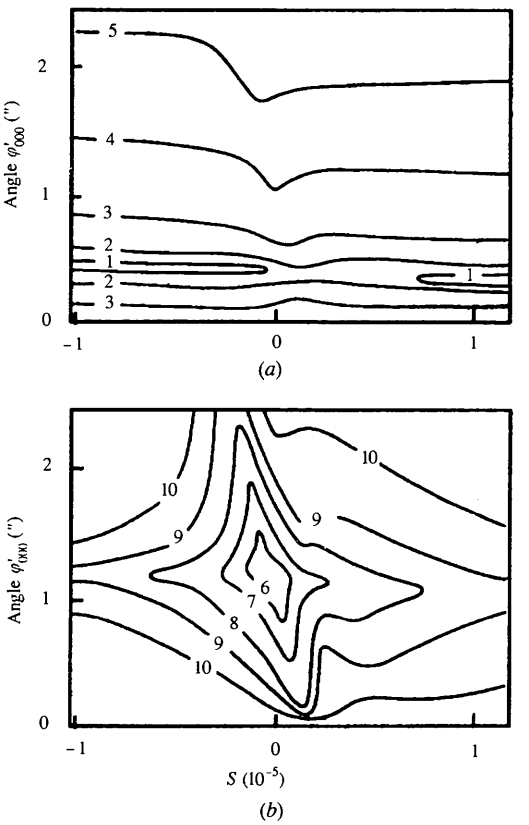

Fig. 5. Reflection coefficient $R_{440}(S, \varphi'_{000})$ for (*a*) σ-polarized and (*b*) π-polarized incident radiation. Levels 1-10 correspond to $R_{440} = 0.3$, 0.2, 0.1, 5×10^{-2}, 2×10^{-2}, 10^{-2}, 5×10^{-3}, 2×10^{-3}, 10^{-3}, 5×10^{-4}, respectively.

within the total-external-reflection region and well collimated within the incident angle φ_{000} only. The actual beam non-monochromaticity and angular divergence were not taken into account in the present calculation. The incident angle is taken to be $\phi_{000} = (|\chi_{000} - \chi_{440}|)^{1/2}$, for which specular reflection coefficient of a diffracted wave in the two-wave case will be the largest. Fig. 5 shows the resulting spectral and angular distribution $R_{440}(S, \varphi'_{000})$. The origin of the angular coordinate φ'_{000} is seen to be shifted with respect to that of φ_{000}, so that $\varphi'_{000} = 0$ for $\phi_{440} = 0$. In the above coordinates, the region of three-wave interaction is seen to exhibit two directions, one parallel to the spectral axis S and the other inclined to it at some angle. A divergence from the $S = 0$ position corresponds to a transition from the three-wave into the two-wave region. Fig. 6 shows semi-integral curves $R_{440}(S) = \int R_{440}(S, \varphi'_{000})\mathrm{d}\varphi'_{000}$. The two-wave diffraction intensities are shown by a dotted line. The shape of the upper curves is characteristic for three-wave diffraction profiles observed in the Renninger experiment arrangement. For the allowed reflection of σ polarization (see Fig. 6*a*), the curve exhibits two regions, one with higher (*Umweganregung*) and the other with lower (*Aufhellung*) intensity as compared with the two-wave case. For the forbidden reflection by π polarization (see Fig. 6*b*), only the higher-intensity region, *i.e.* a peak, occurs.

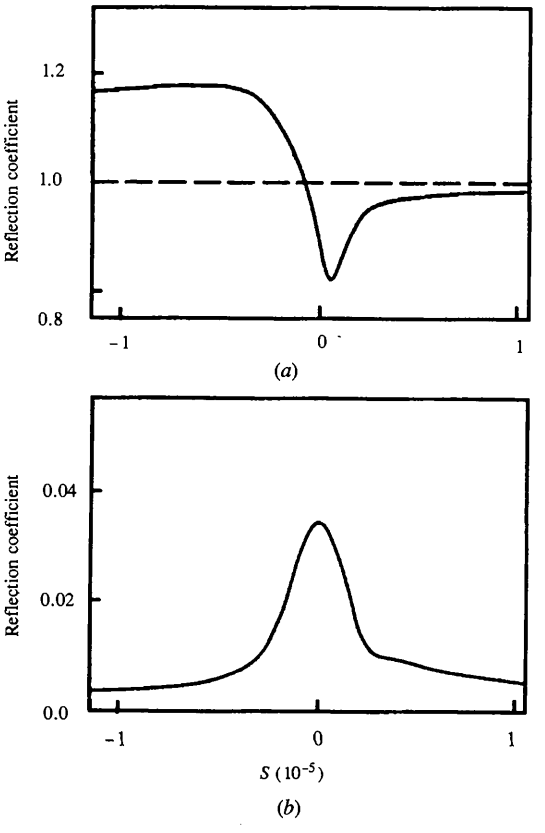

Fig. 6. Semi-integral curves $R_{440}(S)$ for (*a*) σ-polarized and (*b*) π-polarized incident radiation. Values are given in units of $R_{440}(S)$ for the two-wave case for σ-polarized incident radiation.

To conclude, we have proposed a new algorithm that can be used to describe multiple-wave dynamical X-ray diffraction at grazing-angle geometries and have demonstrated the capability of this algorithm in calculating the multiply diffracted *Umweganregung* reflectivities in a polarization-forbidden situation and at grazing incidence and scattering angles. This algorithm is quite general and is not limited to grazing angle but applicable to wide-angle geometries. Moreover, the spectral scanning technique proposed in this paper may facilitate the development of a method for determining lattice parameters and phase invariant of structure-factor multiplets for thin crystal-surface layers utilizing multiple-wave grazing-incidence X-ray diffraction.

References

Andreev, A. V., Gorshkov, M. E. & Ilinskiy, Yu. A. (1985). *Dokl. Akad. Nauk SSSR*, **282**, 69–72. (In Russian.)

Chang, S. L. (1984). *Multiple Diffraction of X-rays in Crystals*, Ch. 2. Berlin: Springer-Verlag.

Colella, R. (1974). *Acta Cryst.* A**30**, 413-423.

Gau, T. S. & Chang, S. L. (1995). *Acta Cryst.* A**51**, 920–931.

Hartwig, J. (1978) *Krist. Tech.* **13**, 1117–1126.

Hung, H. H. & Chang, S. L. (1989). *Acta Cryst.* A**45**, 823–833.

Kishino, S. & Kohra, K. (1971). *Jpn. J. Appl. Phys.* **10**, 551–557.

Kohn, V. G. (1979). *Phys. Status Solidi A*, **54**, 375–384.

Kshevetsky, S. A., Stetsko, Yu. P. & Sheludko, S. A. (1985). *Kristallografiya*, **30**, 468–473. (In Russian.)

Laue, M. von (1931). *Ergeb. Exakten Naturwiss.* **10**, 133–158.

Pinsker, Z. G. (1978). *Dynamical Scattering of X-rays in Crystals*. Berlin: Springer-Verlag.

Renninger, M. (1937). *Z. Phys.* **106**, 141–176.

Stepanov, S. A., Kondrashkina, E. A. & Novikov, D. V. (1991). *Nucl. Instrum. Methods*, A**301**, 350–357.

Stepanov, S. A. & Ulyanenkov, A. P. (1994). *Acta Cryst.* A**50**, 579–585.

Tseng, T. P. & Chang, S. L. (1990). *Acta Cryst.* A**46**, 567–576.

Wagner, E. (1923). *Phys. Z.* **21**, 94–98.